Academic Journal of Science and Technology
ISSN: 2771-3032 | Vol. 10, No. 1, 2024

Optimization Design of Medium-Voltage High-Frequency Transformers Based on Parallel Sampling Kriging Surrogate Model

Chengcheng Yu[1], Laijun Zhao[1, 2, *]

[1]School of Electrical Engineering and Automation, Henan Polytechnic University, Jiaozuo 454003, China
[2]Henan Key Laboratory of Intelligent Detection and Control of Coal Mine Equipment, Jiaozuo 454003, China
[*]Corresponding author: zhaolaijun@hpu.edu.cn

Abstract: In the design process of medium-voltage high-frequency transformers, numerical simulation methods often result in long design cycles and significant computational resource consumption. To achieve rapid and high-precision design for medium-voltage high-frequency transformers, a parallel kriging surrogate model is proposed based on the maximum expected improvement criterion. Initially, Latin hypercube sampling is employed to establish the initial sampling points, and corresponding three-dimensional models of medium-voltage high-frequency transformers are constructed for each sampling point configuration. Finite element simulation software is then used to compute the transformer loss and volume for each model. Subsequently, a kriging surrogate model is developed based on the initial sampling point configuration, and an enhanced parallel sampling strategy is implemented to enhance the fitting accuracy of the kriging surrogate model. Finally, the high-precision kriging surrogate model is utilized as the fitness function for a particle swarm optimization algorithm, with the objectives of minimizing transformer loss and volume. The Pareto optimal solution is sought under multi-objective optimization. The effectiveness of the proposed optimization method is verified through experimental measurements of the loss in a prototype of a medium-voltage high-frequency transformer.

Keywords: Medium-voltage high-frequency transformer, Finite element method, Kriging model, Parallel sampling, Multi-objective optimization.

1. Introduction

With the increasing sales of electric vehicles, the issues of insufficient charging stations and slow charging have become increasingly severe. Conventional power-frequency distribution transformers occupy a large area and have high losses. Moreover, most current fast-charging topologies are unidirectional, meaning that the energy storage of electric vehicles cannot be reversely output to serve the power grid, thus failing to leverage the V2G functionality of future smart grids [1]. Therefore, there is an urgent need to develop novel bidirectional high-power fast charging and discharging power converters. Medium-voltage high-frequency transformers are the core of fast charging and discharging power converters for achieving electrical isolation and energy transfer. The high-frequency operation of transformers greatly reduces the weight and volume of converters. However, the eddy current effects in magnetic cores and windings intensify at high frequencies, leading to increased transformer losses. Moreover, the compact size and structure of high-frequency transformers pose challenges in heat dissipation and insulation design. Additionally, parasitic parameters must be taken into account during high-frequency design. The design of medium-voltage high-frequency transformers requires comprehensive consideration of losses, heat dissipation, insulation, and parasitic parameters. Since it is not possible to optimize all parameters simultaneously, the design of medium-voltage high-frequency transformers presents a multi-objective optimization problem.

Existing transformer design methods primarily consist of the AP design method (area of the product), KG design method (core geometrical constant), and novel artificial intelligence optimization algorithms [2]. The AP and KG methods suffer from low design accuracy and a unidirectional, irreversible design process. If the requirements are not met, calculations need to be restarted from the beginning. Yibo Song [3] utilizes the AP method to design a high-frequency transformer for switching power supplies. Fengjun Liu [4] introduces the calculation process of the KG method and demonstrates a design example of a high-frequency transformer with input and output voltages of 28V and 18V, respectively, and an operating frequency of 40kHz. With the advancement of finite element simulation technology, digital modeling and calculations of transformers through finite element software, coupled with intelligent optimization algorithms, can reduce design iterations and accelerate the design process. Daosheng Liu [5] introduces chaos sequences and adaptive genetic operators into the traditional genetic algorithm, proposing a chaos-adaptive genetic algorithm for the optimized design of amorphous alloy dry-type transformers. Zhan Liang [6] presents an ant lion optimization-based genetic algorithm that optimizes the design of high-frequency pancake transformers under multiple objectives of leakage inductance, temperature rise, efficiency, and power density, taking into account the impact of insulation spacing on the structure. Fugui Liu [7] selects the magnetic core, winding loss calculation model, and AP method formula as optimization objectives, with transformer efficiency as a constraint. It uses adaptive crossover and mutation probabilities to adjust population diversity and improves the MOTO algorithm for the design of high-frequency transformers. However, transformer design involves numerous design variables, constraint boundaries, and objective functions. The algorithm frequently needs to

invoke finite element calculations, leading to exponential growth in computation time and iteration count with the increase in parameter dimensions, significantly affecting the transformer's design cycle.

To reduce the demand for computational resources and time in transformer design using numerical simulation methods, a surrogate-based optimization (SBO) algorithm is employed. This involves approximating a limited number of transformer numerical simulation parameters into a black-box model. Once the model accuracy reaches the required 95%, it is combined with a particle swarm optimization algorithm to achieve global optimization in transformer design. Existing surrogate models primarily include kriging models, radial basis models, support vector regression models, and others. Bin Xia [8] proposes a more effective adaptive collaborative kriging surrogate model by combining two-dimensional finite element analysis with three-dimensional finite element data to optimize the windings of power transformers. Syed Shadab [9] integrates Gaussian process regression models with transformer thermal models to effectively assess transformer lifespan under uncertain conditions. Slawomir Kozuel [10] feeds back the accumulated difference between the target value and the actual target to the kriging model to generate improved predictions, enabling rapid optimization of compact passive components. In summary, surrogate model methods can establish the relationship between target values and input variables through sample data fitting, completing multi-objective optimization tasks for transformers. However, surrogate models often require a large number of samples during training, are prone to overfitting, and have poor generalization capabilities [11]. Therefore, research on how to achieve small-sample fitting of surrogate models and improve model prediction accuracy holds significant value for shortening the design cycle of medium-voltage high-frequency transformers.

To address the aforementioned issues, this paper proposes a parallel-augmentation-based kriging surrogate model for the construction of transformer models with a small sample size. Firstly, a three-dimensional transformer model is established, and its corresponding response values are obtained through finite element analysis using finite element software. Initial sample points and test points are generated using the Latin hypercube sampling method. These initial sample points are then used to construct the surrogate model, and its accuracy is tested. Secondly, based on the parallel augmentation approach, subsequent sample points are selected to maximize the variance while searching the relevant neighborhood of historical optimal points. The surrogate model is rebuilt until the accuracy requirements are met. Finally, the constructed surrogate model is used as the fitness function of the particle swarm optimization algorithm to complete the optimization of medium-voltage high-frequency transformers. Under the same sample size, a comparison is made between the accuracy of the surrogate model before and after parallel augmentation. The effectiveness and accuracy of the proposed method are validated through experimental results from prototype testing.

2. The Optimization Design Method Based on Surrogate Models

2.1. The description of the optimization design problem for medium-voltage high-frequency transformers

The simplified mathematical model for the optimization of medium-voltage high-frequency transformers can be described as follows:

$$min[af(x) + b\varphi(x)], \qquad x_l \le x \le x_u$$
$$g_c(x) \le 0, \qquad c = 1,2,\dots,k$$

In the formula: x is a vector of design variables with dimension; x_l and x_u are the lower and upper limits of the design variable values; f and φ are the objective functions; a and b are the weights of the objective functions; g_i are the constraint conditions.

To reduce computational costs and improve optimization efficiency, surrogate models are often used in place of mathematical models. In this context, the optimization model can be described as follows:

$$min[a\hat{f}(x) + b\hat{\varphi}(x)], \qquad x_l \le x \le x_u$$
$$\hat{g}_c(x) \le 0, \qquad c = 1,2,\dots,k$$

In the formula: $\hat{f}$, $\hat{\varphi}$,and $\hat{g}$ are the approximate response values of the surrogate model.

When optimizing mathematical models, it is necessary to accurately calculate the objective function for each sample, which requires a large amount of computational resources and a long calculation time. However, surrogate models do not have these issues.

2.2. Surrogate modeling method

Surrogate models primarily achieve the replacement of complex systems by establishing mapping relationships between sample inputs and output data, without the need for continuous and complex calculations on the system. The research directions of surrogate models mainly focus on two aspects: one is the data fitting methods of surrogate models, such as kriging models, radial basis function models, support vector regression models, etc.; the other is the selection methods for sample data of surrogate models, such as Latin hypercube sampling, orthogonal experimental design, and the criterion of adding points based on maximum expectation [12]. Both of these aspects directly affect the accuracy and construction speed of the surrogate model. Unlike other surrogate models, the kriging model only requires known sample data and a semi-variogram, without the need for additional parameters or information. The model construction is relatively simple, and based on statistical principles, it can provide information such as confidence intervals and variances of estimated values. Therefore, this paper adopts the kriging method as the fitting approach for the surrogate model.

3. Kriging Surrogate Model Based on Parallel Augmentation

3.1. Latin hypercube sampling

In an n-dimensional space, each one-dimensional coordinate interval is divided into m sub-intervals, and m sampling points are randomly selected from all regions. The selection of the sample point X_{ij} is as follows:

$$X_{ij} = r_i(j) - \frac{U_{ij}(0,1)}{m}, \qquad 1 \le i \le m, 1 \le j \le n$$

In the formula: $r_i(j)$ represents the maximum value of the

ith interval after normalization in the jth dimension; $U_{ij}(0,1)$ is a random number between $[0,1]$.

Considering the advantages of Latin hypercube sampling, such as high sampling rate and good uniformity, 10 initial sampling points for the surrogate model are configured using Latin hypercube sampling, and an additional 10 sampling points are generated to verify the accuracy of the surrogate model.

3.2. Kriging surrogate model

The kriging surrogate model can be represented by the following equation:

$$y = f^{T}(x) \cdot \varphi + z(x)$$

In the formula: $f^{T}(x)$ represents the regression function of x, providing a global approximation model in the design space; φ are the undetermined coefficients of the regression function; $z(x)$ is a random process representing the local deviation based on the global simulation, with an expected value of 0, a variance of σ^2, and a covariance:

$$\mathrm{Cov}\left[z(x_i), z(x_j)\right] = \sigma^2 R(x_i, x_j)$$

In the formula: $R(x_i, x_j)$ represents the variogram between any two sample points, and common variograms include cubic function, Gaussian function, linear function, spherical function, etc. Using the generalized least squares estimation method, the estimated value of φ can be obtained.

$$\hat{\varphi} = (X^{T}R^{-1}X)^{-1}X^{T}R^{-1}Y$$

In the formula: X is the coefficient matrix of the sample points, Y is the response matrix corresponding to the sample points, and σ^2 is the estimated value of .

$$\hat{\sigma}^2 = \frac{1}{N}(Y - X\varphi)^{T}R^{-1}(Y - X\varphi)$$

In the formula: N represents the number of sample points.

Based on the above model parameters, the predicted response value and predicted standard deviation at the prediction point can be obtained as follows:

$$\hat{y}(x_0) = f^{T}(x_0)\varphi + r^{T}(x_0)R^{-1}(Y - X\varphi)$$

$$\hat{s}^2(x_0) = \hat{\sigma}^2\left[1 - r^{T}(x_0)R^{-1}r(x_0) + \frac{\left(1 - XR^{-1}r(x_0)\right)^2}{X^{T}R^{-1}X}\right]$$

In the formula:$r(x_0)$ is the correlation matrix between the sample points and the prediction point.

3.3. Parallel augmentation strategy

Due to the randomness of Latin hypercube sampling, a large number of sample points are required for the surrogate model to achieve the desired fitting accuracy. Selecting sample points based on augmentation criteria can improve modeling efficiency to a certain extent. The Expected Improvement (EI) criterion is an effective global augmentation method. It assumes that the values of the untested points of the objective function follow a normal distribution, i.e., $Y \sim N[\hat{y}(x), s^2(x)]$ is the predicted response value of the kriging model, $s^2(x)$ is the predicted variance, and y_{min} is the current optimal value of the model. Then, the new sample point can be determined as follows:

$$E[I(x)] = \left(y_{min} - \hat{y}(x)\right)\Phi\left(\frac{y_{min} - \hat{y}(x)}{s(x)}\right) + s(x)\psi\left(\frac{y_{min} - \hat{y}(x)}{s(x)}\right)$$

In the formula: $\Phi(\cdot)$ is the cumulative distribution function of the standard normal distribution, and $\psi(\cdot)$ is the probability density function of the standard normal distribution.

The Expected Improvement (EI) augmentation method searches for the sample point with the largest variance, which exhibits strong global search capabilities but slow convergence of model accuracy and weak local search capabilities. In this paper, the historical optimal augmentation criterion is introduced, and the new sample point is determined as follows:

$$F(x) = \alpha_1 y_{min}(1) + \alpha_2 y_{min}(2) + \cdots + \alpha_k y_{min}(k)$$

In the formula: α_k is the weight coefficient, and$\alpha_1 + \alpha_2 + \cdots + \alpha_k = 1$; $y_{min}(k)$ is the optimal value of the surrogate model during the kth fitting iteration.

In this paper, two augmentation criteria are processed in parallel during the modeling process. The historical optimal augmentation method enhances the local search capability of the sample points, complementing the global search capability of the Expected Improvement criterion. The basic flowchart of the parallel augmentation strategy is shown in Figure 1.

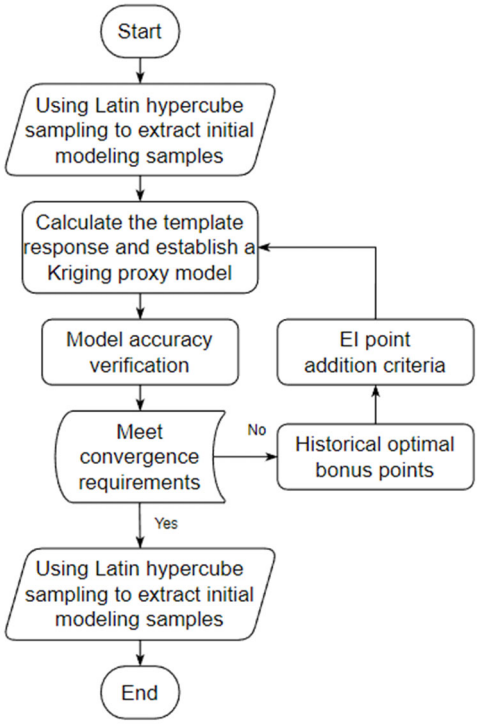

Figure 1. Flowchart

3.4. Convergence criterion

Assuming that the number of test sample points required for the surrogate model is N the true value of the test points is $y_c(x)$, the average value of the true values is $\bar{y}(x)$, and the predicted value of the surrogate model is $y_c^*(x)$, then the accuracy E of the surrogate model can be expressed as:

$$\varepsilon = 1 - \frac{\sum_1^N \left(y_c(x) - y_c^*(x)\right)^2}{\sum_1^N \left(y_c(x) - \bar{y}(x)\right)^2}$$

When building a surrogate model for a medium-voltage high-frequency transformer using the parallel augmentation strategy, a certain level of accuracy $\varepsilon \geq 95\%$ is required.

4. Optimization of Medium-Voltage High-Frequency Transformers

4.1. Model of Medium-Voltage High-Frequency Transformer

The medium-voltage rapid charging and discharging platform is primarily used for electric vehicle charging

stations, and thus has strict requirements on the volume and efficiency of transformers. Therefore, nanocrystalline alloy is selected as the magnetic core material for the medium-voltage high-frequency transformer. The structure of the magnetic core model is shown in Figure 2, and its initial design parameters are presented in Table 1.

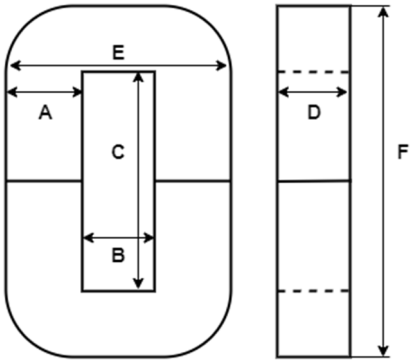

Figure 2. Structure Diagram of the Magnetic Core Model

Table 1. Initial Design Parameters

Design parameter	Numerical value
Core height D/mm	45
Core length F/mm	268
Core width E/mm	145
The core is stacked thick A/mm	50
Window height C/mm	168
Window width B/mm	45
Operating frequency /kHz	100
Number of original side turns	24
Number of secondary side turns	8
Primary side voltage /V	2400
Core weight /kg	9.58
Core volume /cm³	1311.93
Wastage /W	187.79
efficiency	99.62

The three-dimensional simulation model of the nanocrystalline magnetic core transformer established using the finite element method is shown in Figure 3.

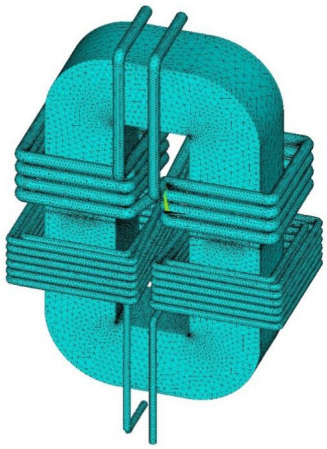

Figure 3. Three-Dimensional Simulation Model Diagram

The design of medium-voltage high-frequency transformers needs to take into account both volume and losses. The volume of the transformer is primarily determined by the size of the magnetic core, which can be represented by the product A_p of the magnetic core window area and the effective cross-sectional area of the magnetic core in the AP method.

$$A_p = A_e A_w$$

In the formula: A_w is the magnetic core window area, and A_e is the effective cross-sectional area of the magnetic core.

The effective voltage on the primary side is U_1:

$$U_1 = N_p \cdot \frac{d\phi}{dt} = N_p \cdot \frac{K_f B_m A_e}{T} \times 10^{-4}$$

In the formula: N_p represents the number of turns; B_m represents the magnetic flux density; ϕ represents the magnetic flux; K_f represents the waveform coefficient.

The utilization coefficient of the magnetic core window area is K_w, the current density is J, and the effective values of the primary and secondary winding currents are I_1 and I_2, respectively:

$$K_w A_w = N_p \cdot \frac{I_1}{J} + N_S \cdot \frac{I_2}{J}$$

From the above equation, we can obtain:

$$A_p = A_e A_w = \frac{U_1 I_1 + U_2 I_2}{4 K_w K_f J B_m A_e f} \cdot A_e \times 10^4$$

In the formula: f is the operating frequency, and U_2 is the effective value of the secondary voltage.

The efficiency of the transformer is $\eta = \frac{P_0}{P_1}$. From this $P_0 + P_1 = \frac{(1+\eta)P_0}{\eta}$, we can derive:

$$A_p = A_e A_w = \frac{(1+\eta)P_0}{4\eta K_w K_f J B_m f} \times 10^4$$

In the formula: P_1 and P_0 are the primary and secondary powers, respectively.

From the above equation, it can be seen that the transformer size is affected by multiple nonlinearly related parameters such as the iron core height, iron core stack thickness, window height, window width, and winding current density.

The losses in a medium-voltage high-frequency transformer are mainly composed of magnetic core losses and winding losses. Among them, the winding losses are much smaller than the magnetic core losses, so they are not discussed in this paper. The classic method to describe the magnetic core losses in high-frequency transformers is the Steinmetz formula, which is as follows:

$$P_c = K f^{\alpha} B^{\beta}$$

In the formula:K, α and β are the Steinmetz coefficients. This method has high accuracy and simple fitting, but it is only applicable to sinusoidal excitation. To facilitate the analysis of magnetic core loss characteristics under other excitations, an improved Steinmetz formula is proposed in reference [13].

$$P_c = F_{eq} K f^{\alpha} B^{\beta}$$

In the formula: F_{eq} represents the magnetic flux waveform coefficient, which is $\pi/4$ for square wave excitation and $2/3$ for triangular wave excitation. It can be seen that the magnetic core losses of a medium-voltage high-frequency transformer are related to material properties and excitation methods.

4.2. Surrogate Model

In this paper, the iron core height (D), iron core stack thickness (A), and window height (C) are selected as optimization variables. The optimization objectives are the iron core volume and transformer losses, with the constraint

conditions being the change in the original design parameters and magnetic flux not exceeding a certain limit. Both the initial 10 sample points and the 10 test sample points are generated using Latin hypercube sampling. The surrogate model prediction accuracy is required to be at level $\varepsilon \geq 95\%$.

Firstly, the initial 10 sample points are used to fit a Kriging surrogate model, and the model is then employed to calculate the predicted values for the test sample points. This gives the current accuracy $\varepsilon^* < 95\%$ of the surrogate model. Subsequently, the particle swarm optimization algorithm is employed to find the sample point where the current optimal objective value of the surrogate model is located. Based on the maximum expected improvement criterion, the point in the sample space that maximizes the variance of the sample data is obtained. These two new sample points, along with the initial sample points, constitute a new sampling space. The above steps are repeated until the accuracy of the fitted surrogate model meets the required standard.

After 21 iterations, the initial sample points are augmented through parallel sampling to obtain a total of 52 sample data points. At this point, the accuracy $\varepsilon^* \geq 95\%$ meets the set precision requirement. The obtained sample points are numbered in sequence from 1 to 52, as shown in Table 2, while the test sample points are numbered from 53 to 62.

Table 2. Surrogate Model Sample Data

ID	Sample 1	Sample 2	…	Sample 51	Sample 52
Core height D/mm	52	40	…	42	50
The core is stacked thick A/mm	55	47	…	53	50
Window height C/mm	148	182	…	144	152
Core volume /cm³	1426.72	1134.88	…	1198.72	1307.60
Wastage /W	187.55	168.34	…	183.62	162.65
efficiency	99.62	99.66	…	99.63	99.67

Using the parallel sampling Kriging surrogate model, the predicted values for the volume and transformer losses of the test sample points numbered 53 to 62 are obtained. A comparison between the predicted and actual values for these two prediction targets is shown in Figure 4. The red line represents the predicted values, while the black line represents the actual values. The prediction accuracy for volume is 95.53%, and the prediction accuracy for transformer losses is 95.01%. These results meet the convergence criteria for the surrogate model and the requirements for transformer optimization design.

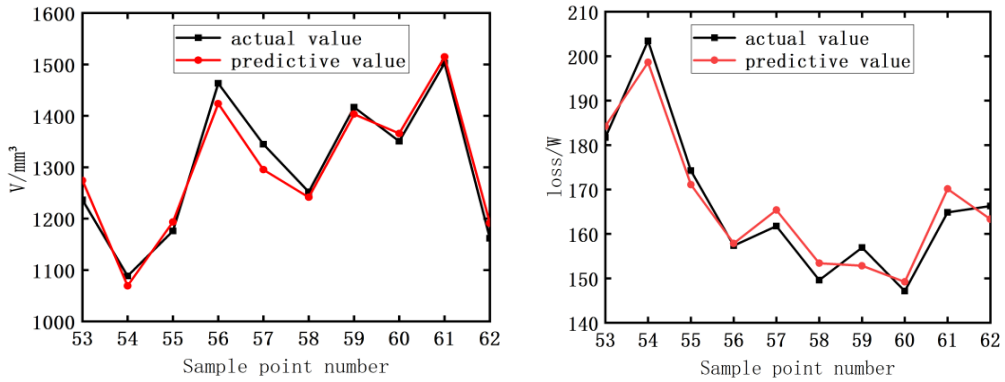

(a) Comparison Chart of Iron Core Volume (b) Comparison Chart of Transformer Losses

Figure 4. Comparison Chart

4.3. Experimental Verification

To verify the superiority of the parallel sampling Kriging surrogate model, the EI method before improvement was used for sampling, and the iteration was performed 42 times. The comparison between the predicted values and actual values obtained is shown in Figure 5. The red line represents the predicted values, while the black line represents the actual values. The prediction accuracy for volume is 78.57%, and the prediction accuracy for transformer losses is 82.56%.

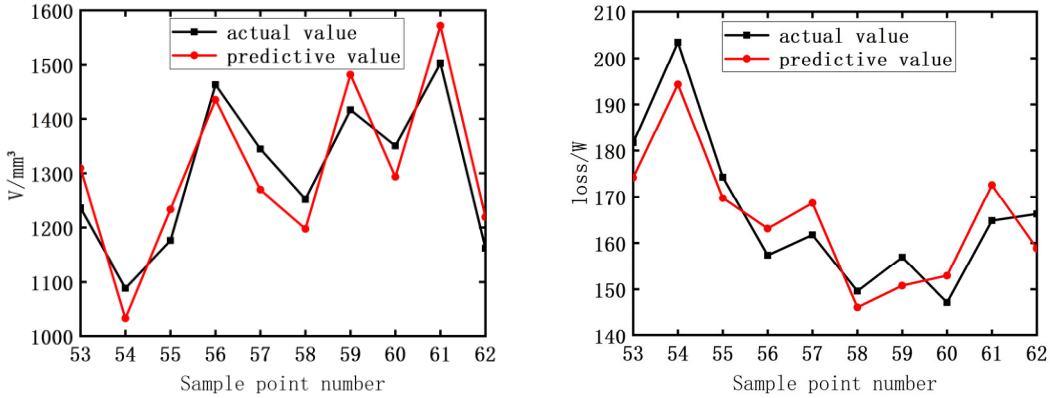

(a) Comparison Chart of Iron Core Volume (b) Comparison Chart of Transformer Losses

Figure 5. Comparison Chart

The surrogate model based on parallel sampling can meet the accuracy requirement after 21 iterations, while the EI

sampling method, after training with the same 52 sample points, exhibits a model accuracy that is approximately 15% lower than the parallel sampling method. The main reason is that the EI sampling method maximizes the variance of the sample points, resulting in a high degree of sample dispersion and slower convergence of fitting accuracy. In contrast, the parallel sampling method incorporates historical optimal points into the samples, constructing a high-precision local surrogate model that satisfies the Pareto frontier. In summary, when constructing a surrogate model for medium-voltage high-frequency transformers, the parallel sampling method exhibits higher fitting accuracy under the same sample conditions.

Acknowledgment

The authors gratefully acknowledge the financial support from the National Natural Science Foundation of China (Project No.52267018) and the Doctoral Fund of Henan Polytechnic University (Project No.B2016-21).

References

[1] Hong Jichao, Liang Fengwei, and Yang Jingsong, et al. “The current status and prospects of the new energy vehicle industry and its technological development, ” in Science & Technology Review, 41nd ed. Vol. 5, 2023, pp. 49-59.

[2] Ye Zhijun, Lin Xiaoming, Tan Kaijia et al. “A review of research on high-frequency transformer technology, ” in Power System Technology, 45nd ed. Vol. 7, 2021, pp. 2856-2870.

[3] Song Yibo and Li Yaowei. “Design of High Frequency Transformer for Switching Power Supply Based on Area Product Method,” in Power & Energy, 40nd ed. Vol. 5, 2019, pp. 543-547.

[4] Liu Fengjun, Modern High Frequency Switching Power Supply Technology and Applications. Beijing: Electronic Industry Press, 2008.

[5] Liu Daosheng, Wei Bokai, Cai Changwan ea al.“Optimization design of amorphous alloy dry-type transformers based on chaotic adaptive genetic algorithm,” in High Voltage Apparatus, 50nd ed. vol. 10, 2022, pp. 40-47.

[6] Liang Zhan, Xie Baochang and Guo Bingtao. “A High Frequency Pie Transformer Optimization Design Based on ALO Algorithm,” in Power Electronics, 55nd ed. Vol. 8, 2021, pp. 1-4.

[7] Liu Fugui, Jiang Jiacheng and Zhao Lin. “Optimization design of high-frequency transformers based on improved MOTO algorithm,” in Electrical Measurement & Instrumentation, 59nd ed. Vol. 8, 2022, pp. 105-111.

[8] Bin Xia, Seokyeon Hong, Kyung Choi, et al. “Optimal Design of Winding Transposition of Power Transformer Using Adaptive Co-Kriging Surrogate Model,” in IEEE Transactions on Magnetics, 53nd ed. Vol. 6, 2017, pp. 7203904.

[9] Syed Shadab, J. Hozefa, K. Sonam, et al. “Gaussian process surrogate model for an effective life assessment of transformer considering model and measurement uncertainties,” in International Journal of Electrical Power & Energy Systems, 134nd ed, 2022, pp. 107401.

[10] Slawomir Kozuel and Anna Pietrenko-Dabrowska. “ Rapid Optimization of Compact Microwave Passives Using Kriging Surrogates and Iterative Correction,” in IEEE Access, 8nd ed. 2020, pp. 53587-53594.

[11] Mohamed A. Bouhlel, Joaquim R. A. Martins. “ Gradient-enhanced kriging for high-dimensional problems,” in Engineering with Computers, 35nd ed, 2019, pp. 157-173.

[12] Fannian Meng, Ziqi Zhang, Liangwen Wang. “Volute Optimization Based on Self-Adaption Kriging Surrogate Model,” in International Journal of Chemical Engineering, 2022, pp. 6799201.

[13] Shen Wei, Wang Fei. “Loss Characterization and Calculation of Nanocrystalline Cores for High-frequency Magnetics Applications,” in IEEE Transactions on Power Electronics, 23nd ed. Vol. 1, 2008, pp. 475-484.